Analysis of the Impact of Inhomogeneous Emissions in the Operational Street Pollution Model (OSPM)

T.-B. Ottosen[1,2], K. E. Kakosimos[1], C. Johansson[3,5], O. Hertel[4], J. Brandt[4], H. Skov[2,4], R. Berkowicz[4], T. Ellermann[4], S. S. Jensen[4], M. Ketzel[4]

[1]{Department of Chemical Engineering, Texas A&M University at Qatar, Doha, Qatar}

[2]{Department of Chemical Engineering, Biotechnology and Environmental Technology, University of Southern Denmark, Odense, Denmark}

[3]{Department of Environmental Science and Analytical Chemistry, Stockholm University, Stockholm, Sweden}

[4]{Department of Environmental Science, Aarhus University, Roskilde, Denmark}

Correspondence to: K. E. Kakosimos (k.kakosimos@qatar.tamu.edu)

[5]{Environment and Health Administration, City of Stockholm, Sweden}

Abstract

Semi-parameterized street canyon models, as e.g. the Operational Street Pollution Model (OSPM®), have been frequently applied for the last two decades to analyse levels and consequences of air pollution in streets. These models are popular due to their speed and low input requirements. One often used simplification is the assumption that emissions are homogeneously distributed in the entire length and width of the street canyon. It is thus the aim of the present study to analyse the impact of this assumption by implementing an inhomogeneous emission geometry scheme in OSPM. The homogeneous and the inhomogeneous emission geometry schemes are validated against two real-world cases: Hornsgatan, Stockholm, a sloping street canyon; and Jagtvej, Copenhagen; where the morning rush hour has more traffic on one lane compared to the other. The two cases are supplemented with a theoretical calculation of the impact of street aspect (height/width) ratio and emission inhomogeneity on the concentrations resulting from inhomogeneous emissions. The results show an improved performance for the inhomogeneous emission geometry over the

homogeneous emission geometry. Moreover, it is shown that the impact of inhomogeneous emissions is largest for near-parallel wind directions and for high aspect ratio canyons. The results from the real-world cases are however confounded by challenges estimating the emissions accurately.

1 Introduction

Semi-parameterized models as e.g. the Operational Street Pollution Model (OSPM®; Berkowicz et al. (1997)) have been frequently applied in cities around the globe over the last 20 years (Assael et al., 2008; Berkowicz et al., 1996; Berkowicz et al., 2006; Ghenu et al., 2008; Gokhale et al., 2005; Hertel et al., 2008; Kakosimos et al., 2010; Ketzel et al., 2012; Kukkonen et al., 2000; Vardoulakis et al., 2005). This type of model has the advantages of low input requirements and short execution times. This means that the model can cover many streets over long time periods due to its low computational demand.

In order to retain the low calculation time of these models, a number of simplifying assumptions have to be made. One assumption, present in e.g. OSPM, is that the emissions are distributed homogeneously over the street canyon in the full length and width of the canyon. However, real streets have traffic lanes with finite width and varying traffic loads, either permanently or as a function of time as e.g. rush hours. Moreover, they might have sidewalks or cycle lanes with no emissions or wide central reserves likewise without emissions. Modelling these situations as homogeneous emission will potentially overestimate one side of the street and underestimate the other side of the street. This has an influence on e.g. limit values, where one side of the street can exceed the limit value while the other doesn't.

Sloping streets represent a natural case of inhomogeneous emissions in that vehicles driving uphill have a higher emission due to the increased engine load compared to vehicles driving downhill. Gidhagen et al. (2004) examined the measured NO_x concentrations from a measurement campaign in Hornsgatan in Stockholm, Sweden; which has a slope of 2.3%, using a Computational Fluid Dynamics (CFD) model. It was shown that the model representation of the wind direction dependence of the concentrations compared to the wind direction dependence of the measurements improved by assuming an emission relationship of 3:1 between the uphill and downhill side of the road. This followed along a marginal improvement in the correlation between the model and the measurements. In Gidhagen et al.

(2004), Kean et al. (2003) is also quoted for reporting markedly higher emissions for vehicles going uphill compared to vehicles going downhill, a feature also implemented in emission models like the Handbook Emission Factors for Road Transport - HBEFA (www.hbefa.net).

Moreover, (Kakosimos et al., 2010) and Vardoulakis et al. (2007) suggested that an improvement in the applicability of semi-empirical street level air quality models could be achieved by implementation of an inhomogeneous emission geometry scheme.

The present study is therefore based on the following research question:

To what extend do the performance of street pollution models like OSPM improve as a result of moving from homogeneous emissions to inhomogeneous emissions, and how is this change influenced by the aspect ratio of the street and the inhomogeneity of the emissions?

The methods applied in the present study are explained in Sect. 2. This is followed by a description of how the concentrations are calculated based on respectively the homogeneous and the inhomogeneous emissions in Sect. 3. The results and discussion are placed in Sect. 4 and the conclusions are presented in Sect. 5.

2 Methods

To analyse the impact of inhomogeneous emissions in OSPM two real-world cases were selected as being representative for inhomogeneous emission geometry streets as found in urban areas. The two real-world cases were supplemented by a set of theoretical calculations to analyse the impact of inhomogeneity and aspect ratio on the results.

The two street canyons chosen to analyse the impact of inhomogeneous emissions were respectively Hornsgatan in Stockholm, Sweden and Jagtvej in Copenhagen, Denmark. The main characteristics of the two street canyons are summed up in Table 1. Hornsgatan is an example of a sloping street canyon with the average slope being 2.3% (Gidhagen et al., 2004), and Jagtvej is diurnally inhomogeneous in that, depending on the time of day, there is more traffic in the northeast direction compared to the southwest direction. Both streets have two driving lanes in each direction (four lanes in total) plus non-emitting areas at the sides. The non-emitting areas are however not modelled explicitly in the present analysis, since including this would require the implementation of horizontal diffusion in the model cf. the discussion in sect. 3.2. This task remains for future work.

In the analysis, the NO_x concentrations were used since in OSPM the concentration of NO_2 is calculated based on the concentration of NO_x and O_3. Thus in order not to add the uncertainties from the chemistry in the analysis, the primary emitted tracer (NO_x) is used. Moreover, previous studies (Ketzel et al. (2011); (Ketzel et al., 2012)) have shown that the emission and dispersion module implemented in OSPM have an acceptable performance for this species.

The years 2007-2009 were chosen for Hornsgatan, since a ban on the use of studded tires was implemented in this street from 2010 and onwards, which probably effected the vehicle distribution. Modelling the influence of this was assessed to be complicated and outside the scope of the present study. For Jagtvej the two years 2003 and 2013 were chosen since traffic counts were performed next to the measurement station in these years. In order to assess the influence of inhomogeneous emissions, accurate traffic input is very important.

Both streets are part of routine air quality control monitoring programs and have been studied extensively in the past. One year of data from Hornsgatan were included in the Street Emission Ceiling Exercise (Larssen et al., 2007; Moussiopoulos et al., 2005; Moussiopoulos et al., 2004) and has thus been subject of a number of modelling studies (e.g. Denby et al. (2013a); Denby et al. (2013b); Johansson et al. (2009); Ketzel et al. (2007); Olivares et al. (2007)). The Jagtvej measurement station is part of the Danish air quality monitoring programme (Ellermann et al., 2013) and has likewise been the subject of extensive analysis (e.g. Ketzel et al. (2011); Ketzel et al. (2012); Silver et al. (2013)).

2.1 Emission modelling and measurements from Hornsgatan

The emission modelling for Hornsgatan uses the hourly automatic vehicle counts for the two driving directions on Hornsgatan. The vehicle counts were made using an inductive loop technology (Marksman 660 Traffic counter and Classifier, Golden River Traffic Ltd., UK). It provides hourly mean total traffic counts, classification of vehicles based on the length of the vehicle, plus mean speed on a lane by lane basis. The automatic counts in the east inner lane were multiplied by 4.2 to compensate for a bias in the counting based on a manual counting check. The exact technical reason for this factor is not known. However, comparison between the Marksman counter and manual counts and between the Marksman counter and automatic camera recordings (Burman and Johansson, 2010) have confirmed the validity of this factor.

The vehicle distribution was modelled as the average weekly vehicle distribution based on vehicle classifications obtained by video number plate recognition in the fall of 2009 (Burman and Johansson, 2010). This ensured that the emission factors reflected the average weekly variation in vehicle distribution. All vehicle categories were modelled using HBEFA 3.2 (www.hbefa.net) except ethanol buses, which do not appear as vehicle category in HBEFA. These were instead modelled using the ARTEMIS emission model (Boulter and McCrae, 2007). The emission factors from ARTEMIS were scaled to a different set of velocities compared to HBEFA. In order to scale the two emission models, the emissions from ARTEMIS were linearly interpolated to match the travel speeds from HBEFA.

The emission factors from HBEFA version 3.2, were used for the emission modelling since this emission model includes the effect of slope on the emissions. The emissions were exported from this model for slopes of +/- 2% and +/- 4% and a linear interpolation to the slope of +/-2.3%, as given by Gidhagen et al. (2004), was performed. In Gidhagen et al. (2004) "Tehran Emission Reduction Project" is cited for reporting uphill emissions being 3-4 times larger than downhill emissions. A significant emission difference between the North and South side of the street can therefore be expected.

The traffic flow situation (called "level of service" in HBEFA) was modelled as a set of discrete categories. This was done by categorizing the individual hour based on the total number of vehicles in the hour. The categorization was performed based on the scheme from the ARTEMIS model reprinted in Table 2.

In setting up OSPM, the street was divided into two emission segments of equal width, although the inhomogeneous emission scheme described in Sect. 3.2 allows for any number of segments, thus each segment covering two traffic lanes. The emissions were distributed over both the lanes and the sidewalk since the modelling of sidewalks is not yet a feature of the model, cf. the discussion in Sect. 3.2. The vehicle speed, used for the calculation of traffic-produced turbulence, was assumed equal to the mean speed between the two lanes comprising the segment.

The emission modelling for Hornsgatan was performed based on two approaches:

- An approach based on the hypothesis that the traffic on the individual lane can be modelled as half the total traffic, subsequently referred to as the "proportional" approach. The inhomogeneity thus only arises from the slope of the street. This

approach is useful if directional- or lane divided traffic counts don't exist for the street in question.

- An approach based on the modelling of inhomogeneous emissions based on traffic counts from the individual lane as described above. This approach is subsequently referred to as the "exact" approach.

The two approaches to emission modelling were subsequently compared.

NO_x was simultaneously monitored on the northern and southern sides of the road with a commercial NO_x chemiluminescence analyser (model 31 M LCD, Environment SA, France). Urban background concentrations were taken from an identical instrument at a monitoring station located on the roof of a building approx. 500 m east of the Hornsgatan street station. The roof level station is representative of the urban background and is not influenced by the emissions in any nearby street canyon.

To analyse if the emission distribution between the north side and the south side of the street can be modelled as a constant ratio, an analysis of measurements for near-parallel (+/- 30°) wind directions for the conditions of a minimum wind speed of $2\frac{m}{s}$ was performed. It was hypothesized that the ratio between the measured concentrations corresponds to the proportions between the emissions. This assumption is of course violated as a result of horizontal dispersion in the street canyon, but this effect was disregarded.

As seen from Fig. 1, the distribution of concentration ratios between the northern and southern side of the street is skewed with the mode being around 1.2 and the mean value being 3.2. This result is not too far from the result presented by Gidhagen et al. (2004), that the emissions at the north side were three times as large as on the south side. Moreover, the distribution is unimodal and has a relatively low standard deviation, which supports the assumption of an even traffic distribution between the north- and the south side of the street.

The hypothesis of a constant ratio distribution will be fortified if the ratio is not changing systematically with time.

The diurnal and weekly variation of the ratio is shown in Fig. 2. As can be seen the values show no clear diurnal or weekly variation and thus the assumption of an even distribution of traffic, but inhomogeneous emissions due to the slope in the two directions, between the two segments seems valid.

2.2 Emission modelling and measurements from Jagtvej

Manual traffic counts next to the measurement station at Jagtvej were performed respectively in 2003 and in 2013. The traffic was counted in two directions on a weekday for 24 hours in 2003 and between 0700-1900 in 2013. The number of vehicles was split into a number of vehicle classes to provide the vehicle distribution. The emissions were modelled using the COPERT 4 model (EEA, 2009).

The diurnal vehicle speed profile for Jagtvej was based on a national study aiming to establish typical diurnal speed profiles for different types of urban streets (TetraPlan A/S, 2001) where the most representative for Jagtvej was chosen. Furthermore, average travel speed data were obtained from a recent national data set (http://speedmap.dk/portal) managed by the Danish Road Directorate. SpeedMap is based on GPS readings from vehicle fleets and provides travel speeds on all major roads in Denmark in a high spatial and temporal resolution. The average vehicle speed from 2011 was used to scale the diurnal profiles from the original study, and the velocity profile was assumed valid for both 2003 and 2013, since no information on the temporal development in vehicle speeds were available within the limits of the present study.

The emissions were subsequently distributed in two segments each covering half of the street width thus both covering the traffic lanes and the sidewalks. The choice of two segments was made since the traffic counts were only distributed into driving directions and not on the individual lane.

The NO_x measurements at the east side of Jagtvej were performed continuously by chemiluminescence using NO_x Aerodyne API instruments. The urban background measurements were measured from a roof level measurement station approximately 500m from the street using similar instrumentation as the street level measurements.

2.3 Theoretical calculations

The resulting concentrations of inhomogeneous emissions as a function of street aspect ratio and emission inhomogeneity were calculated for 360 wind directions with wind speed and total emission approximately similar to the average conditions for Hornsgatan in order to generate comparable results. The calculations were performed on a hypothetical street canyon

with two emission segments each covering half the width of the street. Subsequently the aspect ratio and the emission inhomogeneity were varied over a reasonable interval.

3 Model description

In the following sections the currently applied homogeneous and the tested inhomogeneous emission dispersion schemes will be described. This section does not contain a complete description of the OSPM model, for this the reader is referred to e.g. Berkowicz et al. (1997). However, sufficient details will be provided to understand the modifications in the model regarding handling the emission geometry.

3.1 The homogeneous emission dispersion scheme

To illustrate the modelling principles of OSPM, a typical street canyon situation is illustrated in Fig. 3. OSPM calculates the concentrations (C) at the wall side of the street canyon as a contribution from the street canyon (C_{street}) plus a contribution from urban background concentrations (C_{bg}). The contribution from the street canyon is subsequently a sum of a direct contribution (C_{dir}) plus a recirculating contribution (C_{rec}) (Berkowicz et al., 1997):

$$C = C_{\mathrm{street}} + C_{\mathrm{bg}} \quad (1)$$

$$C_{\mathrm{street}} = C_{\mathrm{dir}} + C_{\mathrm{rec}} \quad (2)$$

It is a fundamental assumption of the model that when the wind blows over a rooftop in a street canyon an hourly averaged recirculation vortex is always formed inside the canyon as illustrated in Fig. 3.

It is assumed that the ground level wind direction inside the recirculation zone is mirrored compared with the roof level wind direction, whereas outside the recirculation zone the wind direction follows the roof level wind direction as illustrated in Fig. 4.

The receptor at the leeward (1) side of the canyon is thus exposed both to a direct contribution from emissions inside the recirculation zone (unless the wind direction is close to parallel as described in Sect. 3.1.1) and a recirculating contribution, and the windward receptor (2) is exposed to a direct contribution from emissions outside the recirculation zone (Berkowicz et al., 1997) and to a diluted recirculating emissions from inside the recirculation zone (Ketzel et al., 2014). In the case where the recirculation zone occupies the whole street canyon, the leeward (marked with “1” in Fig. 5) side of the canyon will be exposed to both a direct and a

recirculating contribution, whereas the windward receptor (marked with "2" in Fig. 5) will only be influenced by the recirculating contribution.

3.1.1 The direct contribution:

The direct contribution can be written on integral form as (Hertel and Berkowicz, 1989):

$$\int_{x_{start}}^{x_{\text{end}}} \frac{dC_{dir}}{dx} dx = \sqrt{\frac{2}{\pi}} \frac{Q}{W\sigma_w} \int_{x_{start}}^{x_{\text{end}}} \frac{1}{x + \frac{u_{street} h_0}{\sigma_w}} dx \quad (3)$$

Where C_{dir} is the direct contribution, x_{start} is the distance from the receptor where the plume has the same height as the receptor, which can also be zero in case $h_r \leq h_0$, and x_{end} is the upper integration limit as defined in Table 3, h_0 is the height of the plume in the wake of a car (usually termed the "initial dispersion"), $h_r$is the height of the receptor (the height of the calculated concentration), Q is the emission flux (in g m^{-1} s^{-1}), W is the width of the street, u_{street} is the street level wind speed, and σ_w is the vertical turbulence flux calculated as a function of the street level wind speed and the traffic produced turbulence.

The integration is performed along a straight line path against the wind direction as illustrated in Fig. 5. Equation (3) is used for calculating the direct contribution on both the leeward side and the windward side; however, the length of the integration paths can differ likewise as illustrated in Fig. 5 .

In Fig. 5 it is assumed that $x_{\text{end}} = L_{\text{rec}}$, the length of the recirculation zone, however, as shown in Table 3 this needs not be the case. The calculation of L_{rec} as a function of the upwind building height (H_u) and the shortening function (f_{red}) is defined in Table 4.

For very long street canyons the plume will start dispersing out of the canyon at the top. In OSPM, this is assumed to happen when the plume height (σ_z) equals the general building height (H_g) (Ketzel et al., 2014) of the canyon. This point is called x_{esc} and is defined as (Hertel and Berkowicz, 1989):

$$x_{esc} = \frac{u_{street}(H_g - h_0)}{\sigma_w} \quad (4)$$

Beyond the point x_{esc} the contribution to the concentration at the receptor is assumed to decay exponentially with distance according to (Hertel and Berkowicz, 1989):

$$\int_{x_{esc}}^{x'_{\text{end}}} \frac{dc_{dir}}{dx} dx = \sqrt{\frac{2}{\pi}} \int_{x_{esc}}^{x'_{\text{end}}} \frac{Q}{u_{street} W H_g} e^{-\frac{\sigma_{wt}}{H g u_{street}}(x - x_{esc})} dx \quad (5)$$

Where σ_{wt} is the roof level turbulence, and x'_{end} is the upper limit of the integral as defined in Table 3. The calculations and definitions of the critical lengths x_{start}, x_{esc}, L_{rec}, and L_{max} are summed up in Table 4.

For close to parallel wind directions the integration length (x_{end}) for the leeward side receptor (1) is extended from L_{rec} to L_{max} to account for concentration resulting from emissions outside the recirculation zone. The calculation of L_{max} as a function of the street width (W), the wind direction with respect to the street axis (θ_{street}), and the length to the end of the canyon is defined in Table 4. The integration is extended when θ_{street} is smaller than 45°, and the contribution to the concentrations from the path outside the recirculation zone is then multiplied by f_{ext} (Hertel and Berkowicz, 1989)[1] :

$$f_{ext} = \cos(2 f_{red} \theta_{street}) \qquad f_{red} = \begin{cases} 1 & ; \quad u_{street} > 2\frac{m}{s} \\ \sqrt{0.5 u_{street}} & ; \quad u_{street} < 2\frac{m}{s} \end{cases}$$

(6) Where θ_{street} is the angle between the street and the street level wind direction.

3.1.2 The recirculating contribution

The recirculating contribution is parameterized as a box model, where it is assumed that the inflow of pollutants equals the outflow of pollutants as illustrated in Fig. 6.

The inflow of pollutants is the emission density in the street multiplied by the integration length L_{base} (Berkowicz et al., 1997):

$$Q_{\text{in}} = \frac{Q}{W} L_{base} \qquad (7)$$

Where $L_{base} = \min(L_{\text{rec}}, L_{\text{max}})$. The recirculation zone is modelled as a trapezium with the upper length being half of the baseline length. The outflow from the box model is thus the ventilation at the top of the recirculation trapezium $(\sigma_{wt} L_{top})$ plus the ventilation at the hypotenuse of the trapezium ($\sigma_{hyp} L_{hyp}$) as illustrated in Fig. 6 (Berkowicz et al., 1997):

$$Q_{\text{out}} = C_{rec}(\sigma_{wt} L_{top} + \sigma_{hyp} L_{hyp}) \qquad (8)$$

[1] In Hertel, O. and Berkowicz, R.: Modelling Pollution from Traffic in a Street Canyon. Evaluation of Data and Model Development., National Environmental Research Institute, 1989. f_{red} is defined as $f_{red} = 0.5 u_{street}$ for $u_{street} < 2\frac{m}{s}$. This has subsequently been changed to $f_{red} = \sqrt{0.5 u_{street}}$ for $u_{street} < 2\frac{m}{s}$.

Where C_{rec} is the recirculating concentration contribution and σ_{hyp} is the average turbulence at the hypotenuse. Equations (7) and (8) can now be solved for the recirculating concentration by setting the inflow equal to the outflow:

$$C_{rec} = \frac{\frac{Q}{W}L_{base}}{\sigma_{wt}L_{top} + \sigma_{hyp}L_{hyp}} \quad (9)$$

3.1.3 Summarizing the dispersion module in OSPM

For regular street canyons (height to width ratio close to one) the recirculation zone will occupy the majority of the canyon. This means that, for a large wind direction interval, the integration length for the leeward receptor will be significantly longer than the integration length for the windward receptor. Furthermore the leeward receptor will be exposed to the full recirculating contribution, while the windward receptor only receives a further diluted recirculating contribution. These two effects mean that the leeward receptor will experience significantly higher concentrations than the windward receptor for a large wind direction interval.

3.2 The inhomogeneous emission dispersion scheme

In order to facilitate the modelling of streets with inhomogeneous emission distributions, the street was divided into a number of parallel segments as illustrated in Fig. 7. The model user will define the width and the emission strength of each segment. At run-time the model calculates several distances (L_{rec}, x_{esc} etc.) that depend on wind flow conditions. The user-defined emission segments are subsequently split into one or more segments with constant emission at these distances. To calculate the concentration from the user-defined and flow generated segments the above presented integrals become divided into a number of integrals and subsequently summed to yield the final concentration. The direct contribution thus becomes:

$$\int_{x_{start}}^{x_{\mathrm{end}}} \frac{dc_{dir}}{dx} dx = \sqrt{\frac{2}{\pi}} \frac{1}{\sigma_w} \sum_{i=n_{start}}^{n_{end}} \frac{Q_i}{W_i - W_{i-1}} \int_{W_{i-1}'}^{W_i'} \frac{1}{x + \frac{u_{street} h_0}{\sigma_w}} dx \quad (10)$$

Where n_{end} is the segment number of the last segment influencing the receptor, n_{start} is the first segment to influence the concentration at the receptor, W_i is the accumulated width of the segment calculated from the receptor, and W_i' is the accumulated width of the segment

calculated along the integration path from the receptor. The segments defined by W_i and W_i' can be either user-defined or dynamically generated.

The exponentially decaying concentration contribution from segments further away than x_{esc} from the receptor becomes:

$$\int_{x_{esc}}^{x'_{\text{end}}} \frac{dc_{dir}}{dx} dx = \sqrt{\frac{2}{\pi}} \sum_{i=n_{start}}^{n_{end}} \frac{Q_i}{u_{street}(W_i - W_{i-1})H} \int_{W'_{i-1}}^{W'_i} e^{-\frac{\sigma_{wt}}{Hu_{street}}(x - x_{esc})} dx \quad (11)$$

The recirculating contribution becomes:

$$C_{rec} = \frac{1}{\sigma_{wt} L_{top} + \sigma_{hyp} L_{hyp}} \sum_{i=n_{start}}^{n_{end}} \frac{Q_i}{W_i - W_{i-1}} (W'_i - W'_{i-1}) \quad (12)$$

In the homogeneous emission scheme the limits of the integrals are determined by the street geometry and the recirculation zone geometry. In the inhomogeneous scheme the limits of the integrals are always W'_{i-1} and W'_i. Instead the limits of the sum determine which segments contribute to the concentration at the receptor.

As seen from the lack of y-dependence in Eq. (3) and (10), the model does not contain expressions for horizontal dispersion. In the original model this was unnecessary since the emissions were homogeneous in the entire canyon. In order to model sidewalks or similar segments with zero emission, horizontal dispersion has to be implemented in the model. This is the case due to the geometry of a canyon with zero emission segments on the sides, meaning that as the wind direction approaches parallel, the integration length quickly approaches zero thus leading to zero concentration as illustrated in Fig. 7. Introducing horizontal dispersion in OSPM was however deemed outside the scope of the present study. In the following cases the streets are therefore divided into segments covering both the traffic lanes and the sidewalks. It would be possible to divide the street into more segments to model the individual traffic lanes. However, either the emission of the inner lane had to be distributed over the sidewalk as well, leading to a too low emission density, or the two lanes would have to be of equal width meaning that the segment division would not correspond to the traffic lane division. To avoid these methodological difficulties, it was decided to model the streets as two segments.

4 Results and discussion

4.1 Hornsgatan

The correlation coefficient (R^2), the Fractional Bias (FB), and the Normalized Mean Square Error (NMSE) for the homogeneous and the exact- and proportional inhomogeneous schemes at Hornsgatan for the years 2007-2009 are shown for the North side receptor in Table 5 and for the South side receptor in Table 6.

As can be seen from Table 5 and Table 6, there is a noticeable change in the performance of the model when moving from homogeneous emissions to inhomogeneous emissions, but only very little between the two approaches for modelling inhomogeneous emissions. This confirms the assumption made in Sect. 2.1 that the emission distribution at Hornsgatan is not, to any significant extend, influenced by diurnal variations. It is also noticeable that the increase in performance is especially pronounced for the North side receptor where the FB is markedly improved and the NMSE is improved as well. For the South side receptor a smaller improvement is seen in FB. Conversely, moving from homogeneous emissions to inhomogeneous emissions has almost zero impact on the correlation coefficient on both sides and only a smaller effect on the NMSE on the north side.

The results are, however, confounded by the modelled street level contributions to the concentrations decline whereas the measured concentrations are almost stable. This effect is especially seen on the North side receptor and to a smaller extend on the South side receptor. This effect can most likely be ascribed to the emission model performance, since the effect is time dependent, and no interannual change in wind speed or direction is found (data not shown). Most likely the emission model is predicting too optimistic reductions for the modern EURO 5/6 vehicles that are not abstained under real-world driving conditions as reported in literature (Carslaw et al., 2011) This is also underlined by the fact that the traffic counts from the inductive loop technology matches fairly well with the camera recordings from 2009. The camera recordings were done over three months where individual cars were identified and compared with register data (Burman and Johansson, 2010). This means that the total traffic counts must be considered reasonably accurate. Since the vehicle distribution for the year 2009 is known very accurately from the camera recordings, this is probably not the explanation either. This leaves a change in traffic flow situation (levels of service) or a difference between the actual and modelled vehicle fleet; in terms of age composition,

emissions as a function of slope, or other factors; over time as possible explanations for this discrepancy.

The wind direction dependency of the concentrations is shown in Fig. 8. As can be seen, the impact of moving from homogeneous emissions to inhomogeneous emissions is largest for parallel wind directions, where each receptor is only exposed to one emission segment. For perpendicular wind directions there is a small difference when the uphill emissions are close to the North side receptor and no difference when it is further away. A similar pattern is seen for the South side receptor with 180° displacement. The wind direction plot shows a noticeable discrepancy between the model and the measurements around 200° for both receptors. Gidhagen et al. (2004) states that horizontal dispersion is underestimated in the applied κ-ε CFD model, and that this is the cause of this discrepancy. If this is the case the underestimation will also appear in the present wind direction plots due to the lack of horizontal dispersion in OSPM.

The weekly variation in concentrations is shown in Fig. 9. The general diurnal variation plus the difference between weekdays and weekends are reproduced well by the model. As can be seen, the two approaches to inhomogeneous emission modelling are almost indistinguishable. It can also be seen from the figure that the impact of inhomogeneous emissions is largest during day time where the concentrations are largest. Figure 9 shows as well that the diurnal variation is not reproduced in detail. On the north side, the morning rush hours and the evening hours are still underestimated, whereas the night time concentrations are underestimated. Moreover, the figure indicates a faster diurnal change in the modelled concentrations as compared to the measured concentrations. This probably has to do with the way the traffic flow situation is modelled as four discrete categories, whereas real traffic will behave like a continuum. This is a potential area of improvement for a future study.

Certain times of the week are also clearly wrong most noticeably Saturday afternoon on the north side receptor and Saturday morning on the south side receptor. This is likewise a potential area of improvement in a future study.

4.2 Jagtvej

The diurnal variation in personal cars and emissions for the two driving directions is shown in Fig. 10. As can be seen the emissions follow the variation in personal cars fairly close. The

deviations between the variations in emissions and number of cars can be explained by the diurnal variation in heavy duty vehicles. The data show the largest inhomogeneity between North and South direction in the morning rush hour. Moreover, the plots show that the traffic and the corresponding emissions have declined substantially from 2003 to 2013.

The diurnal variations in measured and modelled concentrations for weekdays for the two years are shown in Fig. 11. As expected, the change from homogeneous to inhomogeneous emissions only has an influence on the concentrations around rush hour from 8-9 am, where also traffic is inhomogeneous. However the difference between the homogeneous and the inhomogeneous emissions is relatively small, approximately 6 ppb. As also seen from the graph, the model tends to overestimate the emissions in 2003, whereas the 2013 emissions seem fairly correct. The poor model performance for 2003 has to do with the way the model has previously been calibrated to match the measurements. This means that the emissions used in the present study are markedly different from the emissions used when the model was designed. Adapting the model to the new emissions was deemed outside the scope of the present study and an area of improvement for a future study.

The average concentration as a function of wind direction for the morning rush hour for the two years is shown in Fig. 12. As can be seen, the difference between the homogeneous and the inhomogeneous emission is approximately homogeneously distributed among the different wind directions with difference up to 7 ppb. When averaging over the two years, the emission biases equilibrate each other, and give a clearer picture of the wind direction dependency. When looking carefully at the graph it can be seen that the difference in concentration between homogeneous and inhomogeneous emissions is slightly larger for parallel compared to perpendicular directions. The spike in the measurements around 100 degrees is likely a result of a random error, since this spike is not seen in the data for the full diurnal cycle (data not shown). Both the homogeneous and the inhomogeneous emission model have difficulties capturing the measurements from approximately 260° degrees to 360° degrees. From 290 to 345 there is an opening in the street canyon and the difficulties of the model to capture this phenomenon was reported in an earlier study (Ottosen et al., 2015). It was thus deemed outside the scope of the present study to develop a solution to this issue as well.

4.3 Theoretical calculations

A set of theoretical calculations were performed to clearer illuminate the impact of inhomogeneous emissions without the confounding variables influencing the results of the real street canyons. The calculations are performed with a wind speed of 3.5 $\frac{m}{s}$, total emissions of 250$\frac{\mu g}{ms}$, and no urban background concentration. These conditions are corresponding approximately to the average conditions at Hornsgatan. The results of the theoretical analysis of the concentration dependency of the emission inhomogeneity are shown in Fig. 13. As can be seen, a larger emission difference between the two segments also results in a larger difference in concentration. As earlier shown for Hornsgatan, the largest difference is seen for near-parallel wind directions. However, bearing in mind the scale of the y-axis, the differences are small. The inhomogeneity at Jagtvej corresponds to approximately 10 ppb and for Hornsgatan to approximately 20 ppb, orders of magnitude also confirmed by Fig. 8 and Fig. 12. The comparison with measurement will however give a smaller difference, since the real world data are averages of many different wind speeds and emissions.

The impact of the street canyon aspect ratio on the concentrations resulting from inhomogeneous emissions is shown in Fig. 14. The impact is largest for high aspect ratio (building heights larger than street width) canyons. This is expected, since "the street canyon effect", where the impact of the recirculation zone means larger concentrations for the leeward side compared to the windward side, is larger for high aspect ratio canyons. As such, the impact of inhomogeneous emissions will also be larger for high aspect ratio canyons.

5 Conclusions

The present study presented an approach to, and analysed the impact of, implementation of inhomogeneous emissions in a semi-parameterized street canyon model (OSPM). The results were validated against two real world data-sets: One being inhomogeneous as a result of the slope of the street and the other as a result of inhomogeneous directional traffic during rush hours. Moreover, the impact of emission inhomogeneity and street aspect ratio was analysed theoretically.

The results showed that the model including inhomogeneous emissions were better able to reproduce the measured values on the two real-world streets. The impact of the inhomogeneous emissions was largest for the sloping street and the largest effect was seen for

near-parallel wind directions. The results for both streets were however influenced by other factors as well, most likely uncertainties in the emissions, which led to less clarity in the results. Overall the adoption of inhomogeneous emissions leads to a performance increase of up to 15% in fractional bias at the north side receptor of Hornsgatan and a difference in street level contribution of up to 8 ppb. For Jagtvej the difference was shown to be up to 7 ppb in the morning rush hour.

6 Future work

The present study showed a potential for obtaining an improvement in model performance by introducing inhomogeneous emissions in models like OSPM. Two model elements are of immediate interest in relation to the present work:

- At present the receptor is located at the wall of the street. In reality measurement stations are often located several meters from the wall leading to a shorter dilution of the emissions and thereby a higher concentration. Being able to move the receptor freely in the cross-canyon direction could potentially lead to a model performance improvement.
- At present the model does not facilitate the inclusion of zero emission segments such as pedestrian areas. As described in Sect. 3.2, this means that an accurate description of a road like Hornsgatan, where traffic counts exist for all four lanes, is not yet possible. Introducing horizontal dispersion in the model will thus potentially make it possible to describe streets like Hornsgatan more accurately.

Author contribution

T.-B. O., M.K, K. K., C. J., R.B., O. H., and J. B. participated in setting up the study concept and the study design was done by T.-B. O., M.K, K. K., C. J., and R.B. T. -B. O. did the implementation of inhomogeneous emissions in OSPM with input from M. K. and K. K. T.-B. O conducted the data analysis with contributions to analysis and interpretation from M. K., K. K., and C. J. C. J. furthermore provided access to data from Hornsgatan and T. E. provided access to data for Jagtvej. S. S. J. provided input on the traffic profile for Jagtvej. H. S. and K. K. obtained funding for the study. T.-B. O. wrote the article manuscript. All the co-authors participated in the interpretation of the results, provided critical comments to the manuscript, and read and approved the final manuscript.

Code availability

Name of the Software: WinOSPM (Windows version of the Operational Street Pollution Model, OSPM)

Developer: Department of Environmental Science (ENVS), Aarhus University, Denmark

Contact address: Aarhus University, Department of Environmental Science Frederiksborgvej 399, 4000 Roskilde, Denmark.

e-mail: ospm@au.dk

Operational System: Microsoft Windows 7 or later

Software requirements: None

Hardware requirements: At least 100 Mb free hard drive space and 1 Gb RAM

Programming language: Visual Basic 6 combined with linked libraries written in Fortran 77

Availability and cost: WinOSPM is a commercial software requiring licensing. Information on the actual licensing conditions is given on *www.au.dk/OSPM*. A fully functioning 100 days evaluation version can freely be downloaded from this site.

References

Assael, M. J., Delaki, M., and Kakosimos, K. E.: Applying the OSPM model to the calculation of PM_{10} concentration levels in the historical centre of the city of Thessaloniki, Atmospheric Environment, 42, 65-77, 2008.

Berkowicz, R., Hertel, O., Larsen, S. E., Sørensen, N. N., and Nielsen, M.: Modelling traffic pollution in streets, Ministry of Environment and Energy, National Environmental Research Institute, 1997.

Berkowicz, R., Palmgren, F., Hertel, O., and Vignati, E.: Using measurements of air pollution in streets for evaluiation of urban air quality - meteorological analysis and model calculations, The Science of the Total Environment, 189/190, 259-265, 1996.

Berkowicz, R., Winther, M., and Ketzel, M.: Traffic pollution modelling and emission data, Environmental Modelling & Software, 21, 454-460, 2006.

Boulter, P. and McCrae, I.: Assessment and reliability of transport emission models and inventory systems, TRL Limited, 2007.

Burman, L. and Johansson, C.: Utsläpp och halter av kväveoxider och kvävedioxid på Hornsgatan, Environment and Health Administration, SLB-analys, 2010.

Carslaw, D. C., Beevers, S. D., Tate, J. E., Westmoreland, E. J., and Williams, M. L.: Recent evidence concerning higher NO_x emissions from passenger cars and light duty vehicles, Atmospheric Environment, 45, 7053-7063, 2011.

Denby, B. R., Sundvor, I., Johansson, C., Pirjola, L., Ketzel, M., Norman, M., Kupiainen, K., Gustafsson, M., Blomqvist, G., Kauhaniemi, M., and Omstedt, G.: A coupled road dust and surface moisture model to predict non-exhaust road traffic induced particle emissions (NORTRIP). Part 2: Surface moisture and salt impact modelling, Atmospheric Environment, 81, 485-503, 2013a.

Denby, B. R., Sundvor, I., Johansson, C., Pirjola, L., Ketzel, M., Norman, M., Kupiainen, K., Gustafsson, M., Blomqvist, G., and Omstedt, G.: A coupled road dust and surface moisture model to predict non-exhaust road traffic induced particle emissions (NORTRIP). Part 1: Road dust loading and suspension modelling, Atmospheric Environment, 77, 283-300, 2013b.

EEA: EMEP/CORINAIR Atmospheric Emissions Inventory Guidebook, Chapter on Exhaust Emissions from Road Transport. Methodology for COPERT 4., European Environmental Agency, 2009.

Ellermann, T., Nøjgaard, J. K., Nordstrøm, C., Brandt, J., Christensen, J., Ketzel, M., Jansen, S., Massling, A., and Jensen, S. S.: The Danish Air Quality Monitoring Programme - Annual Summary for 2012, Arhus University, DCE - Danish Centre for Environment and Energy, 2013.

Ghenu, A., Rosant, J.-M., and Sini, J.-F.: Dispersion of pollutants and estimation of emissions in a street canyon in Rouen, France, Environmental Modelling and Software, 23, 314-321, 2008.

Gidhagen, L., Johansson, C., Langner, J., and Olivares, G.: Simulation of NO_x and ultrafine particles in a street canyon in Stockholm, Sweden, Atmospheric Envrionment, 38, 2029-2044, 2004.

Gokhale, S. B., Rebours, A., and Pavageau, M.: The performance evaluation of WinOSPM model for urban street canyons of Nantes in France, Environmental Monitoring and Assessment, 100, 153-176, 2005.

Hertel, O. and Berkowicz, R.: Modelling Pollution from Traffic in a Street Canyon. Evaluation of Data and Model Development., National Environmental Research Institute, 1989.

Hertel, O., Hvidberg, M., Ketzel, M., Storm, L., and Stausgaard, L.: A proper choice of route significantly reduced air pollution exposure - A study on bicycle and bus trips in urban streets, Science of The Total Environment, 389, 58-70, 2008.

Johansson, C., Norman, M., and Burman, L.: Road traffic emission factors for heavy metals, Atmospheric Environment, 43, 4681-4688, 2009.

Kakosimos, K. E., Hertel, O., Ketzel, M., and Berkowicz, R.: Operational Street Pollution Model OSPM) - a review of performed application and validation studies, and future prospects, Environmental Chemistry, 7, 485-503, 2010.

Kean, A. J., Harley, R. A., and Kendall, G. R.: Effects of Vehicle Speed and Engine Load on Motor Vehicle Emissions, Environmental Science & Technology, 37, 3739-3746, 2003.

Ketzel, M., Berkowicz, R., Hvidberg, M., Jensen, S. S., and Raaschou-Nielsen, O.: Evaluation of AirGIS: A GIS-based air pollution and human exposure modelling system, International Journal of Environment and Pollution, 47, 226-238, 2011.

Ketzel, M., Hertel, O., Ottosen, T.-B., Kakosimos, K., and Berkowicz, R.: Validation of New Parameterisations for the Operational Street Pollution Model (OSPM). In: Proceedings of Abstracts 9th International Conference on Air Quality - Science and Application, University of Hertfordshire, Hatfield, United Kingdom, 2014.

Ketzel, M., Jensen, S. S., Brandt, J., Ellermann, T., Olesen, H. R., Berkowicz, R., and Hertel, O.: Evaluation of the Street Pollution Model OSPM for Measurements at 12 Streets Stations Using a Newly Developed and Freely Available Evaluation Tool, Journal of Civil & Environmental Engineering, S:1, 2012.

Ketzel, M., Omstedt, G., Johansson, C., Düring, I., Pohjola, M., Oettl, D., Gidhagen, L., Wåhlin, P., Lohmeyer, A., Haakana, M., and Berkowicz, R.: Estimation and validation of $PM_{2.5}/PM_{10}$ exhaust and non-exhaust emission factors for practical street pollution modelling, Atmospheric Environment, 41, 9370-9385, 2007.

Kukkonen, J., Valkonen, E., Walden, J., Koskentalo, T., Karppinen, A., Berkowicz, R., and Kartastenpää, R.: Measurements and modelling of air pollution in a street canyon in Helsinki, Environmental Monitoring and Assessment, 65, 371-379, 2000.

Larssen, S., Mellios, G., van den Hout, D., Kalognomou, E. A., and Moussiopoulos, N.: Street Emission Ceiling (SEC) exercise - Phase 3 report, 2007. 2007.

Moussiopoulos, N., Kalognomou, E. A., Papathanasiou, A., Eleftheriadou, S., Ph, B., Ch, V., Samaras, Z., Mellios, G., Vouitsis, I., Larssen, S. E., Gjerstad, K. I., F.A.A.M, K.D, Teeuwisse, S., and Aalst, R. v.: Street Emission Ceiling exercise -- Phase 2 report, 2005. 2005.

Moussiopoulos, N., Kalognomou, E. A., Samaras, Z., Mellios, G., Larssen, S. E., Gjerstad, K. I., F.A.A.M, K.D, and Teeuwisse, S.: Street Emission Ceiling exercise -- Phase 1 report, 2004. 2004.

Olivares, G., Johansson, C., Ström, J., and Hansson, H.-C.: The role of ambient temperature for particle number concentrations in a street canyon, Atmospheric Environment, 41, 2145-2155, 2007.

Ottosen, T.-B., Ketzel, M., Skov, H., Hertel, O., Brandt, J., and Kakosimos, K.: A Parameter Estimation and Identifiability Analysis Methodology Applied to a Street Canyon Air Pollution Model, Environmental Modelling & Software, Submitted, 2015.

Silver, J. D., Ketzel, M., and Brandt, J.: Dynamic parameter estimation for a street canyon air quality model, Environmental Modelling & Software, 47, 235-252, 2013.

TetraPlan A/S: Standardværdier for trafikdata til OSPM modellen, TetraPlan A/S, 2001.

Vardoulakis, S., Gonzales-Flesca, N., Fisher, B. E. A., and Pericleous, K.: Spatial variability of air pollution in the vicinity of a permanent station in central Paris, Atmospheric Environment, 39, 2725-2736, 2005.

Vardoulakis, S., Valiantis, M., Milner, J., and ApSimon, H.: Operational air pollution modelling in the UK - Street canyon applications and challenges, Atmospheric Environment, 41, 4622-4637, 2007.

Vägverket and SMHI: Dokumentation ARTEMIS i SIMAIR, Vägverket och SMHI, 2007.

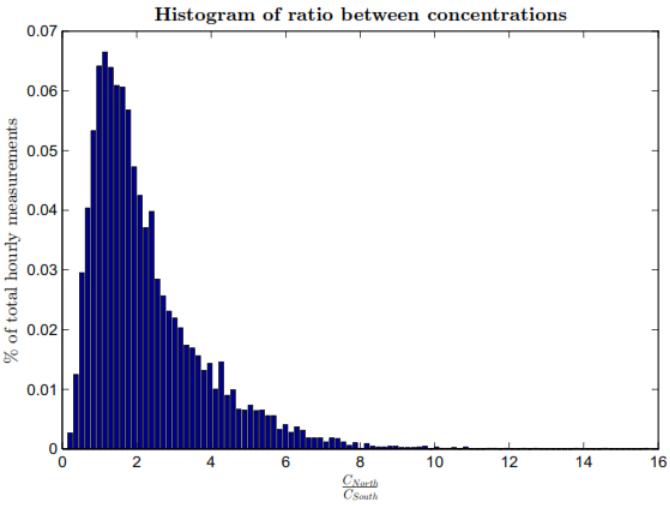

Figure 1 Histogram of ratio between North- and South side receptor for near-parallel wind directions for Hornsgatan, Stockholm.

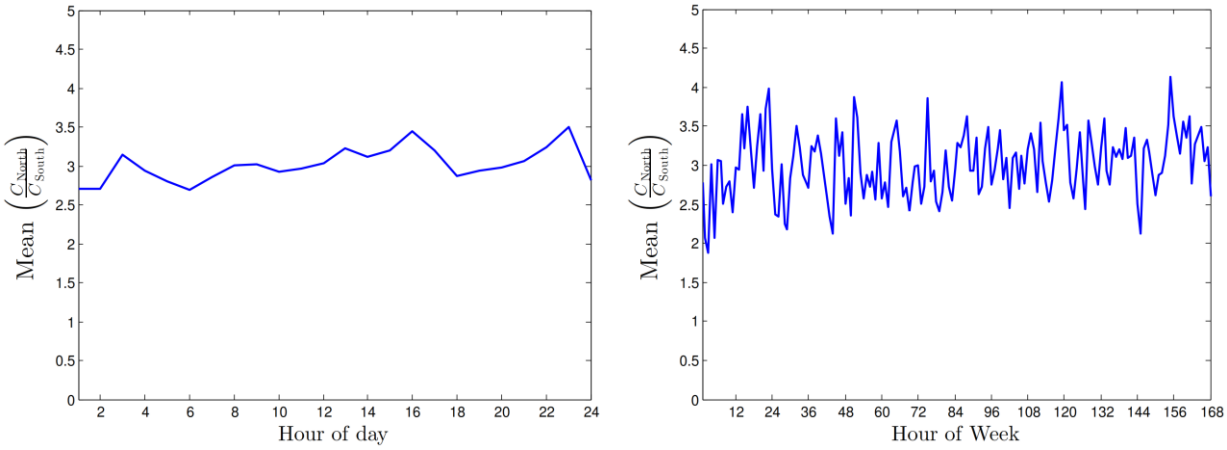

Figure 2 Diurnal and weekly variation in the mean ratio between the concentrations for the north- and south side receptor for near-parallel wind directions with wind speeds above 2 $\frac{\text{m}}{\text{s}}$ for Hornsgatan, Stockholm.

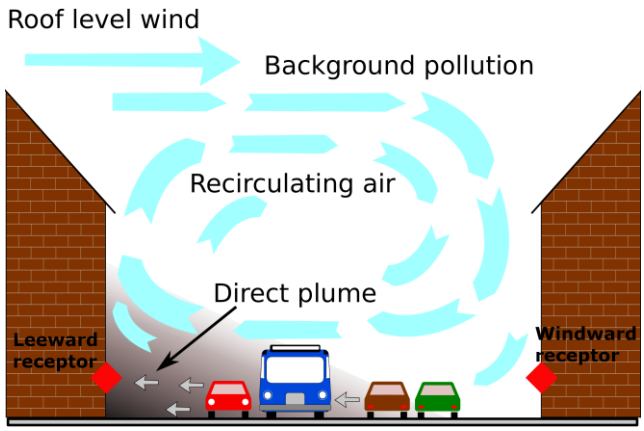

Figure 3 Cross-section of a street canyon. The figure illustrates the governing flow patterns as modelled in OSPM. The two receptors are marked with red diamonds. In the figure the recirculation zone occupies the whole canyon although this need not be the case as e.g. shown in the following figures. Figure modified from Silver et al. (2013).

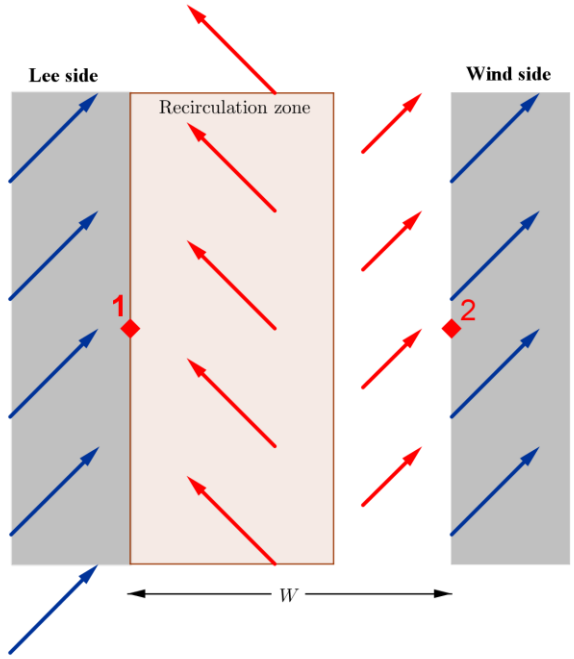

Figure 4 Schematic view of a street canyon seen from the top. The arrows represent the wind directions as modelled in OSPM. The length of the arrows are not proportional to the wind speed. The blue arrows are rooftop wind directions and the red arrows are street level wind directions. The receptors are marked with red diamonds.

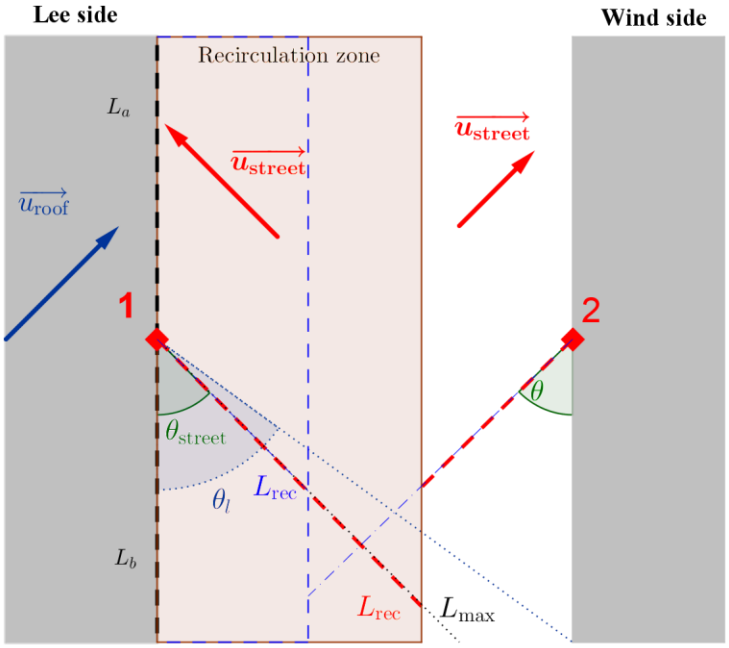

Figure 5 Illustration of the integration paths (red dotted lines) for an arbitrary wind direction for the two receptors in the canyon. The upper blue dotted line marks a critical wind direction (θ_l) which affects the calculation of the integration path length, and L_b is the length to the end of the canyon used to calculate the maximum integration length (L_{max}). L_{rec} is the length of the recirculation zone. A second recirculation zone is illustrated in blue with the new integration lengths likewise plotted with dotted blue lines.

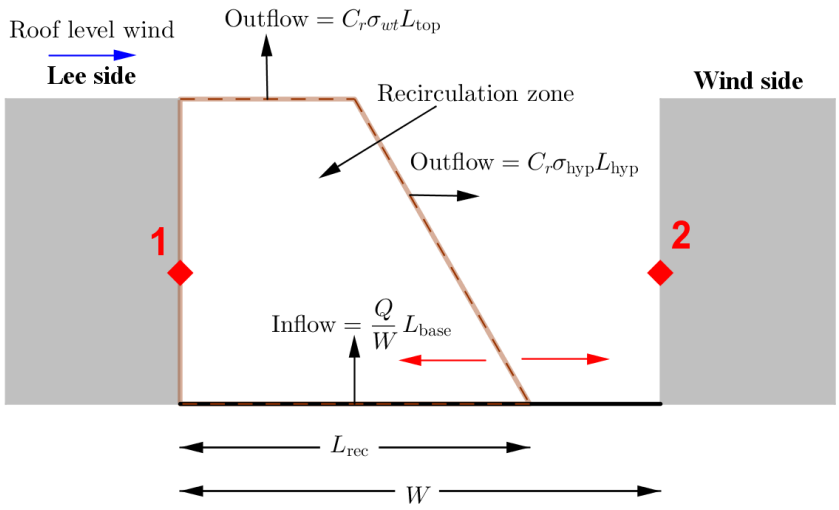

Figure 6 Cross-section of a street canyon with the dimensions of the recirculation zone illustrated. The red arrows represent the street level wind direction. Based on (Hertel and Berkowicz, 1989) p. 69

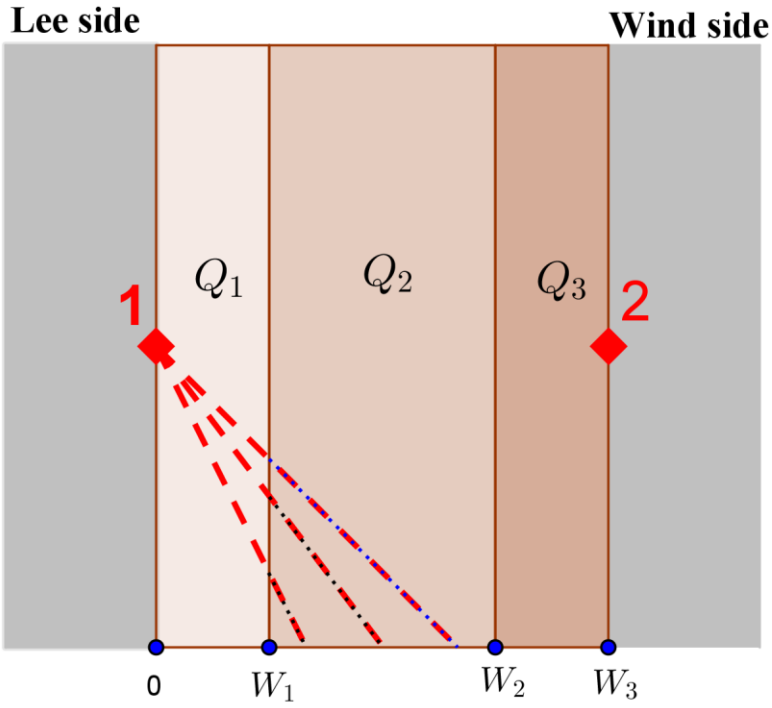

Figure 7 Illustration of the division of the street canyon into a number of segments with accumulated widths W_1, W_2, W_3,… and emission strengths Q_1, Q_2, Q_3, … The red dotted lines represent the integration path for receptor 1 for different wind directions. The blue dotted lines represent the contribution from segment Q_2.

1

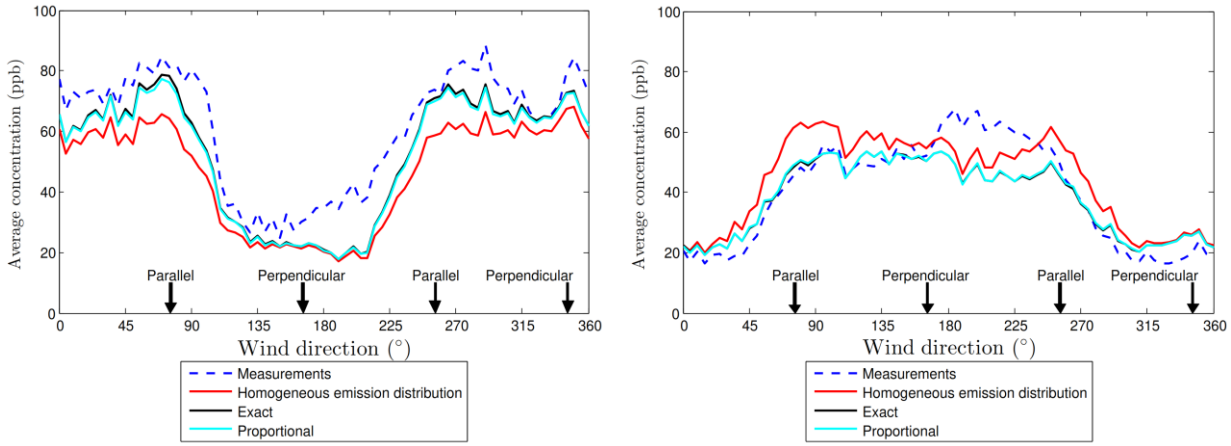

1

2 Figure 8 Mean NO_x concentrations as a function of wind direction for the period 2007-2009
3 for the North side receptor (left side) and the South side receptor (right side). Where the black
4 curve is hardly visible it is identical to the cyan curve.

5

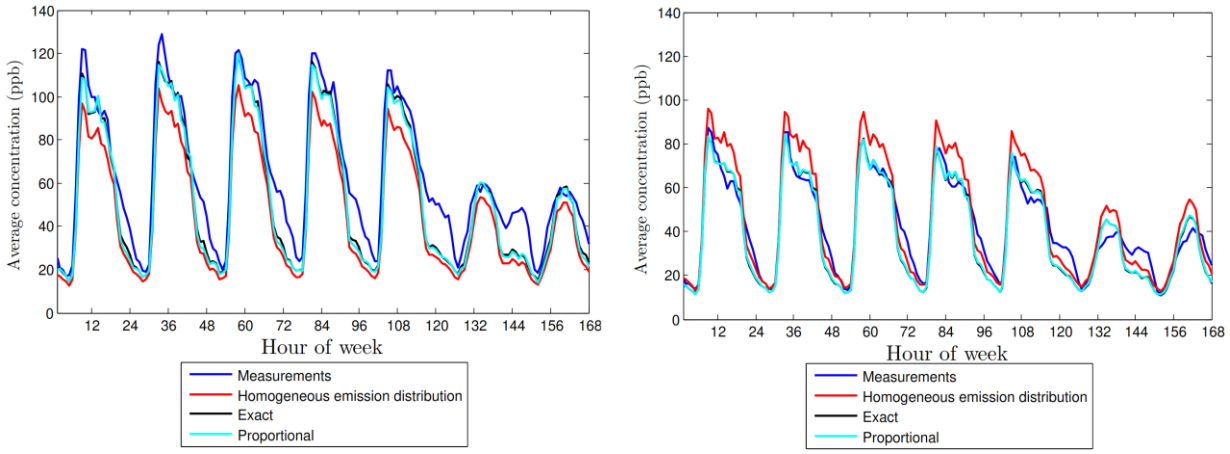

Figure 9 Weekly variation in NO_x concentrations for the period 2007-2009 for the North side receptor (left) and the South side receptor (right). Where the black curve is not visible it is below the cyan curve.

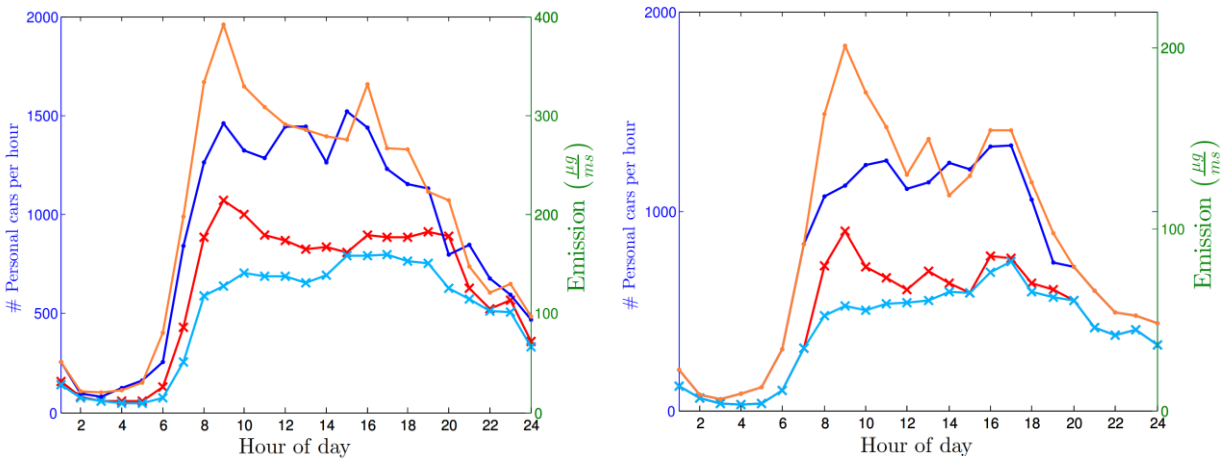

Figure 10 Diurnal variation for weekdays in personal cars per hour and total NO_x emissions for for all vehicles for 2003 (left) and 2013 (right). The red and orange graphs are for the northeast direction and the blue graphs are for the southeast direction. The curves marked with dots are the emissions and the curves marked with crosses are the number of personal cars per hour.

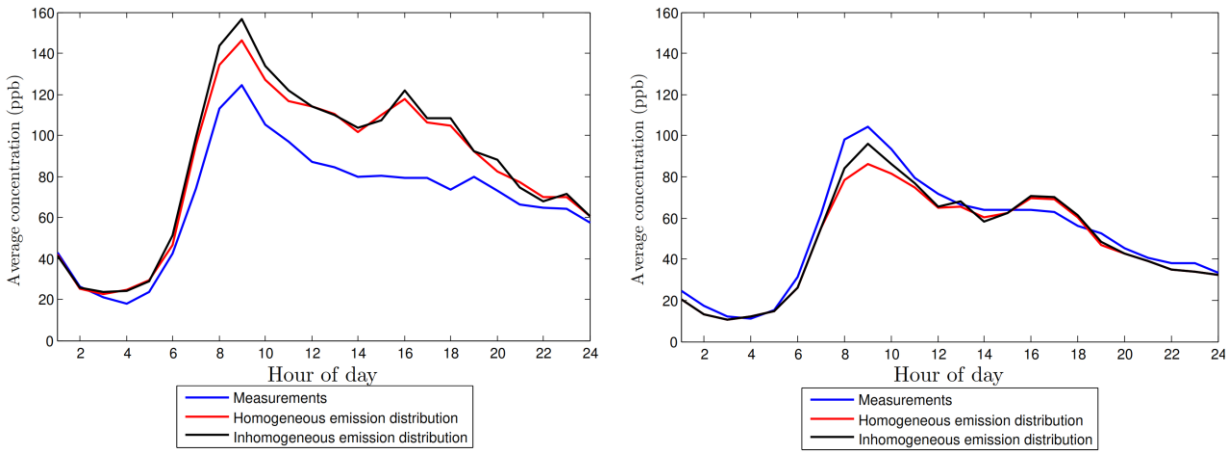

1

2 Figure 11 Diurnal variation in NO_x concentrations on weekdays for 2003 (left) and 2013
3 (right).

4

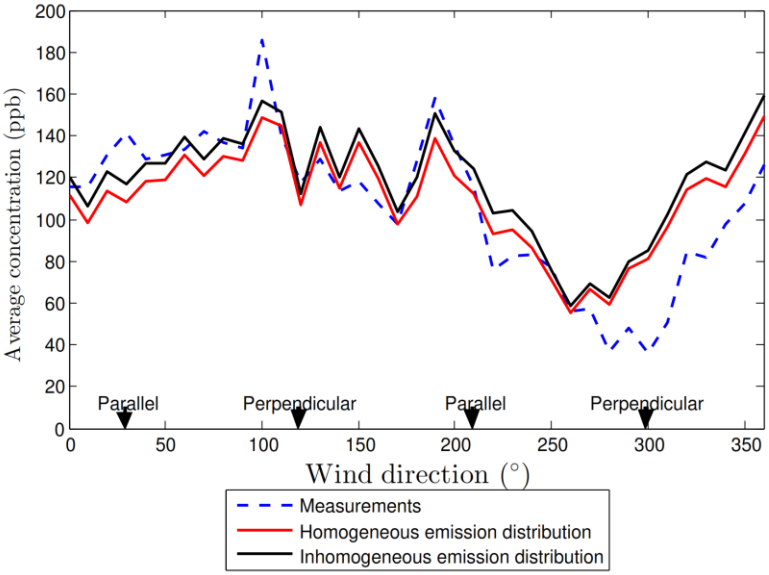

Figure 12 Average NO_x concentrations as a function of wind direction for the morning rush hour 7am-9am for both 2003 and 2013.

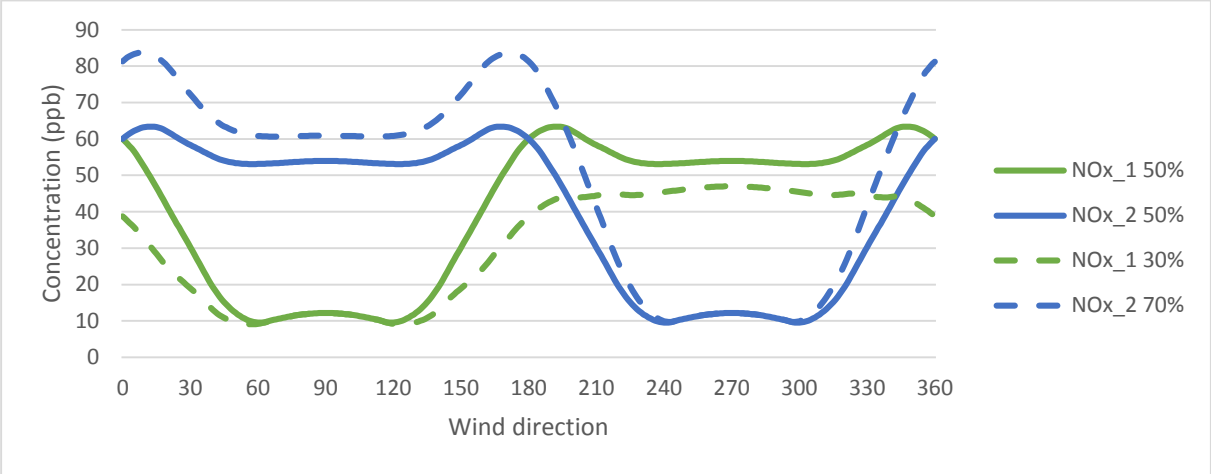

Figure 13 Theoretical calculation of the concentration for the two receptors for a street canyon with two emission segments each covering half the street width and an aspect ratio of one as a function of the emission inhomogeneity and wind direction. Receptor 1 is marked with green colour and receptor 2 is marked with blue colour. The inhomogeneity is given as percentages of the total emission for the two segments and the inhomeneous case is marked with dotted lines.

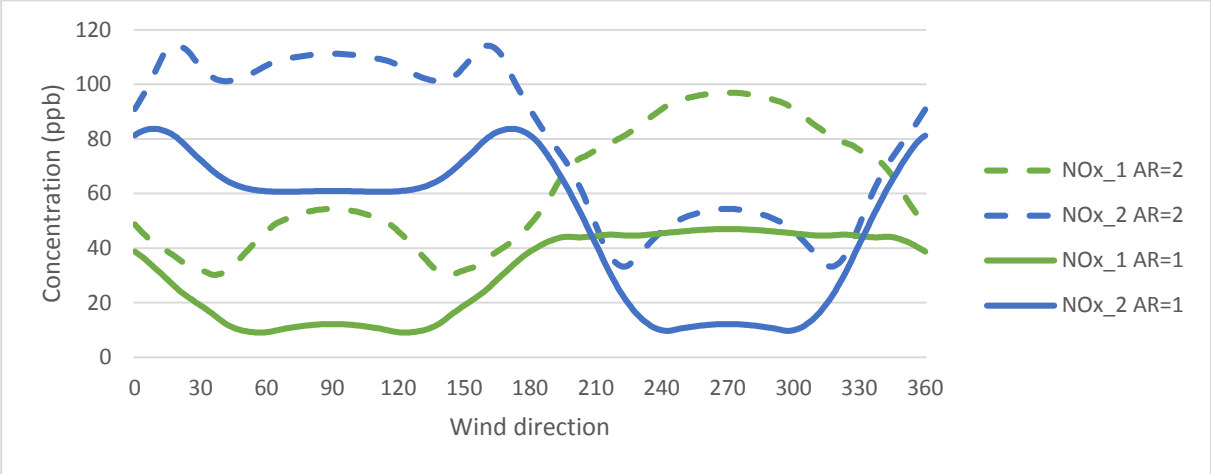

Figure 14 Theoretical calculation of the concentration for the two receptors for a street canyon with an emission inhomogeneity of 70% (north going) / 30% (south going) as a function of aspect ratio (AR) and wind direction. Receptor 1 is marked with green colour and receptor 2 is marked with blue colour. The case with high aspect ratio is marked with dotted lines.

Table 1 Overview of the properties of the two street canyons used for validation of the dispersion schemes in the study. There is a measurement station (receptor) at each side of the street in Hornsgatan, but only one measurement station on the East side of Jagtvej.

Name:	Hornsgatan	Jagtvej
City	Stockholm	Copenhagen
Country	Sweden	Denmark
Latitude	55° N	59° N
Width	24m	25m
Height	24m	22m
Years in analysis	07, 08, 09	03, 13
Street orientation	76°	30°
Average daily traffic	35.500	20.000
Mean vehicle speed (km/h)	45	29
Heavy duty share	4%	3%
Receptor height	3.0m(North) 3.3m(South)	3.6m (East)

Table 2 Level of service as a function of total number of vehicles per hour based on (Vägverket and SMHI, 2007)

Level of service	Total number of vehicles per hour
Freeflow	<601
Heavy	601 – 899
Saturated	900 – 1399
Stop + Go	>1400

Table 3 Table of upper integration limits for respectively Eq. (3) (x_{end}) and Eq. (5) (x'_{end}). The definition and calculation of the lengths can be found in Table 4.

Magnitude:	x_{end}	x'_{end}
$L_{\text{rec}} > x_{esc} > L_{max}$	L_{max}	-
$L_{\text{rec}} > L_{max} > x_{esc}$	x_{esc}	L_{max}
$x_{esc} > L_{\text{rec}} > L_{max}$	L_{max}	-
$x_{esc} > L_{max} > L_{\text{rec}}$	L_{rec}	-
$L_{max} > x_{esc} > L_{\text{rec}}$	L_{rec}	-
$L_{max} > L_{\text{rec}} > x_{esc}$	x_{esc}	L_{rec}

Table 4 Table of the critical lengths along the integration path. These lengths determine the upper and lower limit of the integrals in the homogeneous emission dispersion scheme and of the sums in the inhomogeneous emission dispersion scheme. Moreover, they determine if the dispersion should be calculated according to Eq. (3) or Eq. (5) plus whether the concentration should be multiplied with f_{ext} as defined in Eq. (6). f_{red} is the shortening function as defined in Eq. (6), H_u is the upwind building height, θ_{street} is the wind direction compared to the street direction, θ_l is the critical wind direction as illustrated in Figure 5, $W$is the street width, $L_b$is the length from the receptor to the end of the street as illustrated in Figure 5, and h_r is the height of the inlet of the receptor above street level.

Name:	**Expression:**			**Description:**
$\boldsymbol{L_{\mathrm{rec}}}$	$2 \cdot f_{red} \cdot H_u$			Length of the recirculation zone
$\boldsymbol{x_{esc}}$	$\frac{u_{street}(H_g - h_0)}{\sigma_w}$			Length where the plume starts to disperse vertically out of the canyon.
$\boldsymbol{x_{start}}$	$\frac{u_{street}(h_r - h_0)}{\sigma_w}$	;	$h_r \geq h_0$	Length where the vertical dispersion of the plume equals the height of the receptor.
	0	;	$h_r < h_0$	
$\boldsymbol{L_{\mathrm{max}}}$	$\frac{W}{\sin(\theta_{street})}$	;	$\theta_{street} > \theta_l$	Maximum integration path length.
	$\frac{L_b}{\cos(\theta_{street})}$	;	$\theta_{street} < \theta_l$	

Table 5 Correlation coefficient, Fractional Bias, and Normalised Mean Square Error for the years 2007-2009 for the North side receptor. "Exact" and "Proportional" refer to the emission modelling approaches described in section 2.1. Moreover, the measured and modelled annual mean NO_x concentrations for the individual years are also shown. These are calculated as local street contribution only i.e. the background concentration subtracted from the measured/modelled street concentration to reflect the street contribution.

	Measured	Homogeneous emissions	Inhomogeneous emissions	
			Exact	Proportional
Correlation coefficient (R^2)		0.85	0.85	0.85
Fractional Bias (FB)		-0.30	-0.16	-0.17
Normalised Mean Square Error (NMSE)		0.36	0.26	0.26
Annual mean 2007 (ppb) (ΔC)	56.8	44.3	53.0	51.3
Annual mean 2008 (ppb) (ΔC)	53.9	37.7	44.2	44.2
Annual mean 2009 (ppb) (ΔC)	53.9	35.0	40.5	40.2

1 Table 6 Statistical quantities for the South side receptor. Same definitions as in Table 5.

	Measured	Homogeneous emissions	Inhomogeneous emissions	
			Exact	Proportional
Correlation coefficient (R^2)		0.83	0.84	0.84
Fractional Bias (FB)		0.08	-0.08	-0.07
Normalised Mean Square Error (NMSE)		0.27	0.28	0.28
Annual mean 2007 (ppb) (ΔC)	32.7	41.2	33.1	33.6
Annual mean 2008 (ppb) (ΔC)	34.5	37.2	31.0	31.0
Annual mean 2009 (ppb) (ΔC)	34.6	34.5	29.1	29.2

2

3